STUDY OF AN ELECTROOPTIC SENSOR FOR HIGH-VOLTAGE MEASUREMENTS

J. C. SANTOS, L. PINHEIRO C. SILVA, J. C. J. ALMEIDA
Escola Politécnica da Universidade de São Paulo EPUSP–Depto. de Energia e Automação Elétricas-PEA – Laboratório de Sistemas Ópticos - LSO
Av. Prof. Luciano Gualberto Trav.3 No158, CEP:05508-900 São Paulo, SP - Brasil

J. RUBINI JR, N. M. ABE, A. PASSARO
Instituto de Estudos Avançados-IEAv/EFA/LEV
Rodovia dos Tamoios km 5,5 - Putim, CEP: 12.228-001, São José dos Campos, SP - Brasil

Abstract. *In the recent years, several optical potential transformers (OPT) have been developed and applied to perform high-voltage measurements in electrical power systems. Such devices offer very attractive advantages, compared to conventional transformers, such as, fast transitory response, low susceptibility to electromagnetic interference, high signal/noise ratio, reduced size and weight, and provide complete electric isolation between high-voltage system and measurement equipment. A very important part of an OPT is the high-voltage optical sensor, which is usually based on an electrooptic sensor. The design of high-voltage electrooptic sensors is a difficult task, often demanding aid of electromagnetic simulation tools to be precisely done. This work illustrates the effect of different crystal sizes on the performance of a multi-segmented electrooptic sensor with several pieces of electrooptic crystals and with single electrooptic crystal in longitudinal configuration. The electric field is computed by applying a 2D Finite Element Method (FEM) exploiting the geometric axial symmetry presented by the sensor. The method allows evaluation of the* V_π *voltage, which is related to the dynamic range and is often used as a figure of merit for the electrooptic sensor. A fine adjustment of* V_π *voltage for a given application can be obtained by choosing carefully the type, number, shape, and position of electrooptic crystals. The resulting values of the* V_π *voltage obtained by simulation, for different lengths of single electrooptic crystals in a given configuration of electrooptic sensor are compared with the results obtained by an experimental arrangement. Such comparison shows a good agreement between the two sets of values, demonstrating the usefulness of the FEM simulation method as an eletrooptical sensor designing tool.*

Keywords: *optical high voltage sensor, high voltage measurements, finite element method, electric field, electrooptic material*

1 Introduction

In the last few years, innovative electrooptic sensors, such as Optical Potential Transformers (OPTs) and Optical Current Transformers (OCTs), have been developed and used for high-voltage and high-current measurements in electrical power systems. As attractive advantages, compared to conventional transformers, this kind of sensor presents fast transitory response, low susceptibility to electromagnetic interference (EMI), high signal/noise ratio, reduced size and weight. Moreover, they provide complete and reliable electric isolation between high-voltage power equipment and low-voltage measurement equipment, improving the reliability of entire electric system.

The core of these devices, the high-voltage optical sensor, is often built exploring the electrooptic effect, i.e., the modification of electric permittivity that certain materials (electrooptic materials) present when submitted to an external electric field [1]. As the propagation characteristics of electromagnetic radiation in crystals is governed by the electric permittivity, a good estimative of the electric field inside the electrooptic crystal is of main interest for the design of any electrooptic device, including extrinsic electrooptic sensors built using optical fibers and electrooptic materials.

In this work, a study of the performance of multi-segmented electrooptic sensors [2][3][4], with several pieces of electrooptic crystals and with a single electrooptic crystal [4] in longitudinal configuration, is presented. The electric field is computed by applying a 2D Finite Element Method (FEM) code, which exploits the geometric axial symmetry presented by the sensor [5]. This code has been used for finite element analysis (FEA) of several optic integrated components based on electrooptic effects [6][7]. For the single electrooptic crystal configuration, in section 5, the computed V_π voltages are compared to experimentally obtained values.

2 The Electrooptic Sensor

An electrooptic sensor used for high-voltage measurements in power systems is based on the concept of longitudinal electrooptic modulator [8][9]. Fig. 1 shows an amplitude modulator composed by one single electrooptic crystal.

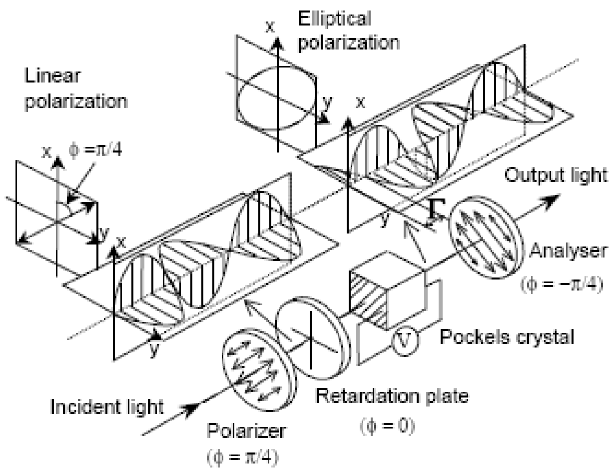

Fig. 1 - A longitudinal electrooptic modulator: the source V generates an electric field in the direction of the light propagation.

In the longitudinal configuration an electric field parallel to the light beam propagation direction is imposed to the crystal. This type of modulator performs an integration of the electric field along the propagation direction of the light, which is equivalent to a potential difference.

For a polarimetric modulator in longitudinal configuration, the applied field induces a phase retardation Γ of the light beam. The total phase retardation, Γ_t, is the summation of electrically induced phase retardation (Γ) plus an additional retardation caused by a plate retardation of $\pi/4$ (ϕ_r) and is given by

$$\Gamma_t = \phi_r + \pi \cdot \frac{V}{V_\pi}, \tag{1}$$

where V_π is called half-wave voltage of the modulator and is defined as the value of V at which Γ reaches to π [1][10][11]. The value of the V_π voltage determines the sensitivity and linearity of the electrooptic sensor.

The transmitted light intensity T (transmission factor), as a function of the applied voltage $V(t)$ is given by

$$T = \frac{I_o}{I_i} = sin^2\left(\frac{\pi}{4} + \frac{1}{2} \cdot \pi \cdot \frac{V(t)}{V_\pi}\right), \tag{2}$$

where I_i and I_o are the light intensities at input and output sides of the modulator, respectively

The characteristic curve of response for a pockels longitudinal modulator is shown in Fig. 2.

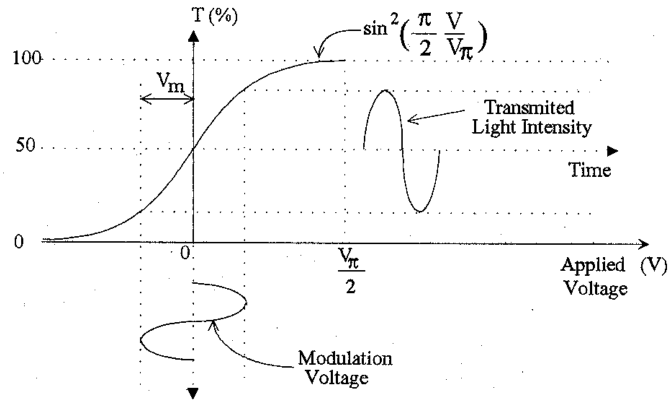

Fig. 2 - Pockels modulator response curve.

The multi-segmented electrooptic sensor is an assemblage of several electrooptic crystals and a mechanical support of dielectric material, which maintains the crystals spaced by air gaps as shown in Fig. 3. In previous works [2][9], the V_π voltage for multi-segmented sensors was estimated by the expression:

$$V_\pi = \frac{(\lambda.K)}{2\,.\,n_0^3\,.\,r_{41}\;n\,.\,d_1}, \tag{3}$$

$$K = \left[n\,.\,d_1 + \frac{\varepsilon_1}{\varepsilon_2}(n-1)\,.\,d_2\right] \tag{4}$$

where λ is the wavelength of the laser light source, n_0 is the ordinary refractive index, r_{41} is the pockels coefficient of the crystal, n is the number of crystal pieces, d_1 is the thickness of the electrooptic crystals, d_2 *is* the thickness of the air gaps, ε_1 is the permittivity of the crystal and ε_2 the permittivity of the dielectric support material. Equation (4), however, is not valid in general (regarding the shape and size of the electrooptic crystal pieces). Usually, an equivalent value of K, that allows a better estimative of V_π, can be obtained from the voltage applied to the electrodes and the mean electric field inside the crystals:

$$K = \frac{V}{\overline{E}_1} \tag{5}$$

where:

$$\overline{E}_1 = \frac{1}{n}\sum_{i=1}^{n} E_{1(i)} \tag{6}$$

and $E_{1(i)}$ is the mean electric field computed in each crystal piece.

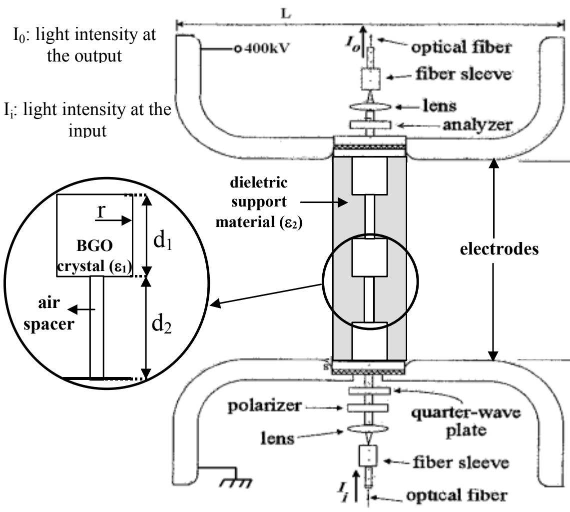

Fig. 3 - A longitudinal multi-segmented electrooptic modulator: electric field in the direction of the light propagation, I_i.

3 Computational analysis

The computational analysis adopted in this work uses the finite element method (FEM) to compute the electric field in the electrooptic crystals, which is used in Eq.(6). In another work [12] a standard genetic algorithm was used to optimize the number and distribution of crystal slices in order to obtain a specified V_π value.

3.1 The finite element method

FEM is extensively used in Engineering to solve problems that can be represented by one or more differential partial equations. The accuracy of the FEM solutions for elliptical equations is well established. The computation of the electric field in the electrooptic sensor involves the solution of the Poisson equation [13] [14].

4 Experimental Setup

The optical sensor was assembled to the ac high-voltage signal processor and the whole set subjected to tests conducted to measure its performance with respect to the voltages applied to it. Figure 4 illustrates the Optical Sensors Laboratory facilities at Escola Politécnica of University of São Paulo (LSO-PEA/EPUSP), used for the essays, and the sensor interferometer connected to a high voltage transformer, rated 80.5 kV, 7.5 kVA.

Fig. 4 - Sensor interferometer of the OPT connected to the high-voltage transformer at Optical Sensors Laboratory.

Figure 5 shows the block diagram of the OPT, including the signal processor unit developed for demodulating the ac high-voltage applied to it. The detailed description of the signal processor was published in another article [15].

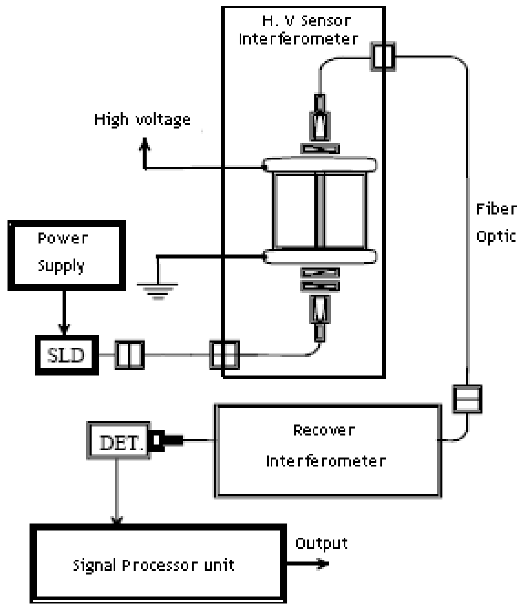

Fig. 5 – shows the block diagram of the electronic arrangement of sensor.

Table I shows the experimental V_π / λ values for six lengths of crystals.

TABLE I Experimental V_π / λ values

BGO crystal thickness	V_π / λ values
100 mm	6.15E+10 V/m
70.6 mm	7.54E+10 V/m
30.4 mm	2.1E+11 V/m
18.8 mm	3.38E+11 V/m
13.3 mm	4.73E+11 V/m
10.2 mm	7.97E+11 V/m

5 Results

The computational results presented in this work were obtained considering BGO crystals ($Bi_4Ge_3O_{12}$ - Bismuth Germanate) as electrooptic material. The relevant physical properties of this material are n_0 = 2.098 (the ordinary refractive index) and r_{41} = 1.03×10^{-12} m/V (the Pockels coefficient), $\varepsilon_1 = 16\varepsilon_0$, where ε_0 is the permittivity of the vacuum. The voltage between the electrodes of the sensor was assumed equal to 400 kV and the sensor is installed inside a grounded metallic cylindrical tank.

5.1 Analysis of a single crystal sensor

In Fig. 6 the mean electric field and the V_π / λ parameter are shown as a function of the BGO thickness (d_1), for crystals of radius (r) equal to 0.5 mm. Both the electric field and V_π vary considerably for electrooptic crystals with thicknesses from 1 to 12 mm, and particularly in the range from 1 to 3 mm. Figure 6 also shows the experimentally obtained V_π / λ values, presented in Table I.

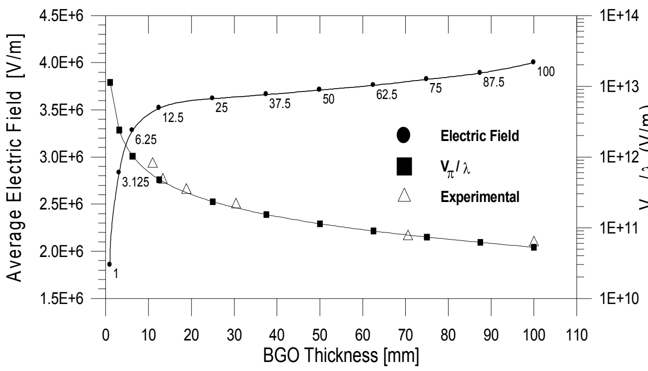

Fig. 6 – Average electric field and V_π / λ as a function of the crystal thickness (single crystal sensor).

As can be seen in Fig. 6, experimental and calculated V_π / λ values are in very close agreement, differing only by less than 3%.

Figure 7 presents a comparison of the variation of the electric field along the axial axis inside two crystals, one with radius r equal to 2.5 mm and the other with 0.5 mm. In both cases, the crystal thickness is of 7.5 mm and it is positioned near the electrode of 400 kV. The computed V_π / λ values are, approximately, $1.0\ 10^{12}$ V/m for r = 2.5 mm and $7.1\ 10^{11}$ V/m for r = 0.5 mm.

Notice that both the thickness and the radius of the electrooptic crystal are important design parameters of this kind of sensor.

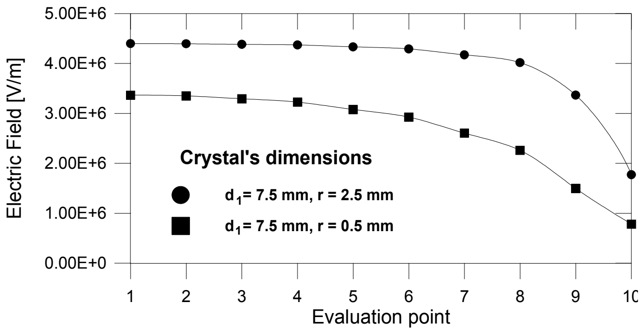

Fig. 7 – Comparison of the electric field variation inside crystals of same thickness and different radius. The curves show the electric field in 10 points inside the crystal and along the axial axis.

5.2 Analysis of multi-segmented sensors

The results obtained for two different configurations of the multi-segmented sensor are presented. Eight BGO crystals are positioned between the electrodes, numbered from 1 to 8. The positions 1 and 8 are the closest to the energized electrode and to the grounded electrode, respectively. Table II shows the characteristics of the sensoring cell for these configurations. For the meaning of the parameters d_1, d_2, and r, refer to Fig. 3.

Configuration 1 corresponds to the multi-segmented sensor presented in [2][3] and [5]. The value of V_π, estimated by Eqs. (3) and (4) is very accurate in this case. In fact, it differs less than 3% from the one obtained by using the equivalent K, Eq.(5) it is also evaluated the effect of the presence of a grounded metallic ring in the vicinity of the sensor on the electric field along the optical path (symmetry line). Two cases were considered for a sensor with electrodes of 160 mm of diameter. In the first case, the ring presents an inner diameter of 100 mm and an outer diameter of 120 mm. In the second case, the inner and the outer diameters are 50 mm and 70 mm, respectively. The height of the rings is 40 mm. The metallic ring alters the electric field along the optical path, but this modification has small effect on V_π. As a matter of fact, the V_π values obtained in these cases are 6.996 MV and 6.917 MV, respectively.

Figure 8 illustrates the variation of V_π / λ as a function of the diameter of the sensors electrode.

TABLE II Sensoring cell characteristics

	Configuration 1	Configuration 2
d_1	1.0 mm	7.5 mm
d_2	14.5 mm to 16.0 mm	~5.72mm
ε_2	$2.7\varepsilon_0$	$3.6\varepsilon_0$
r	5 mm	0.5 mm

A study of the effect of the crystal radius was also performed, based on the Configuration 1. Figure 9 illustrate the mean electric field in each crystal position for sensors built with crystals of different radius. Notice that crystal radius has a strong influence on V_π, as shown in Fig. 10, and can be used to achieve a fine-tuning in sensor's design.

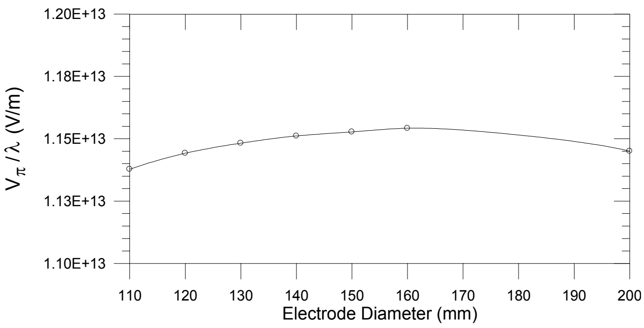

Fig. 8 – Configuration 1 - V_π / λ as a function of the electrode diameter.

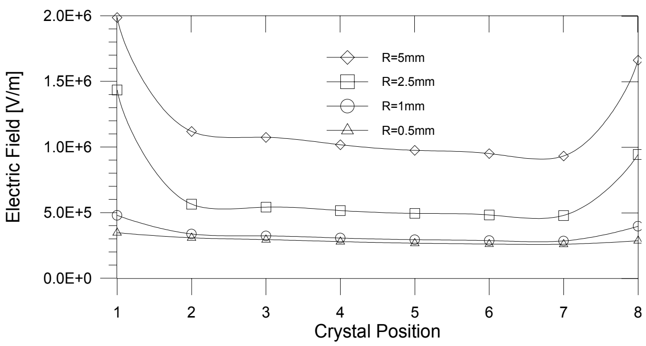

Fig. 9 – Mean electric field inside each one of the 1 mm thick slices for sensors composed by crystals of different radius.

In Configuration 2 the electric field varies considerably inside each one of the electrooptic crystals and Eq.(4) is no longer valid. In fact, the value of K presents 80% of discrepancy compared with the one computed from Eq.(5) and the FEM. Figure 11 shows the electric field obtained for different electrode sizes as a function of the BGO crystal position for Configuration 2. The modification of the electric field in the crystals, caused by a grounded metallic ring in the vicinity of a sensor with electrode diameter of 110 mm is also presented. In this case, the ring presents inner and the outer diameters of 50 mm and 70 mm, respectively, and height of 40 mm. The V_π voltage as a function of the electrode diameter is presented in Fig. 12. Notice that the V_π / λ values differ only by less than 1%. The value of V_π / λ with the influence of the metallic ring is of $9.71\text{x}10^{11}$, and also differs by less than 1% of the value obtained without the ring.

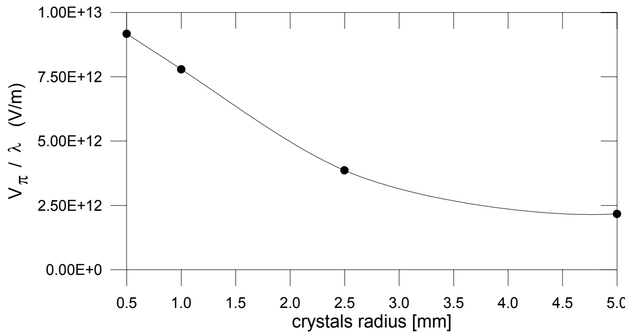

Fig. 10 - V_π voltage as a function of the crystal radius for the configuration 1.

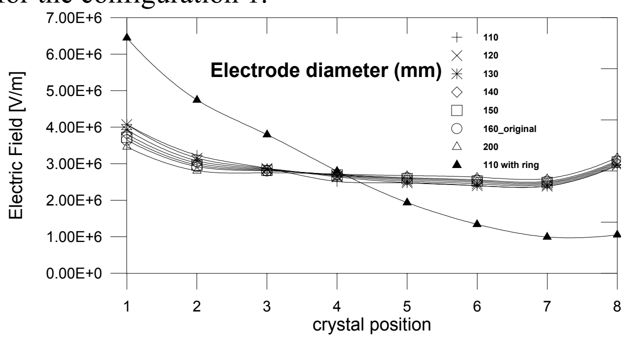

Fig. 11 - Mean electric field in the BGO crystals for Configuration 2.

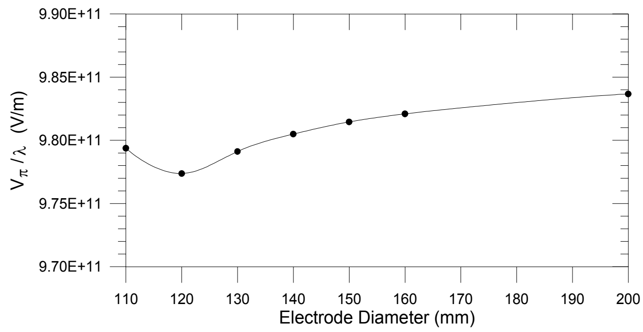

Fig. 12 - Configuration 2 - V_π / λ as a function of the electrode diameter.

6 Conclusions

In this work an approach for the design of multi-segmented electrooptic sensors suitable for high-voltage measurement is presented.

The effect of the size of the electrooptical crystals and of other geometric parameters were studied. It was evidenced that, in the range of parameters considered, the electrode diameter has small influence on the definition of V_π value. The electrode dimensions must to be defined in order to achieve desired dielectric strength.

Following the previous conclusion, the dimensions of the sensor were fixed in the optimization process in order to improve a sensor prototype previously developed. Only the position and size of the electrooptic material, as well as the geometry of the electrooptic crystals support were allowed to vary. Several configurations of the sensor nucleus were obtained attaining the objective imposed.

A very important result of this work is the evidence that experimental and calculated V_π / λ values are in close agreement, differing only by less than 3%. This result clearly demonstrate that FEM simulation method is useful as a valuable designing tool for eletrooptical sensors development.

In a future work, it is planned the application of the same technique to reduce the size of the sensor and to solve some problems associated with assemblage of the device.

Acknowledgements
The authors would like to extend their thanks to Fundação de Amparo à Pesquisa do Estado de São Paulo - FAPESP and to Instituto de Estudos Avançados - IEAv for the technical support to undertake this work .

References

[1] Yariv A. & Yeh, P. *Optical Waves in Crystals*, John Wiley New York, USA, 1984.

[2] Santos, J.C., 1996. *New Optical Pockels Techniques for Direct Measurement of High Voltage*, PhD Thesis, Tokio University, Japan.

[3] Santos, J.C.; Taplamacioglu, M.C.; and Hidaka, K.; *Optical High Voltage Sensors Using Pockels Fiber Crystals*, Proceedings of 10th International Symposium on High Voltage Engineering, Montreal, Canada, Vol. 4, pp. 475-478, Aug. 25-29 (1997)

[4] Rubini, J.J.; Passaro A.; Abe, N. M., & Santos J.C., *Design Study of an Electrooptic Sensor for Pulsed High-Voltage Measurements*. Proceedings of the XXVI Iberian Latin-American Congress on Computational Methods in Engineering – CILAMCE 2005, Guarapari, Espírito Santo, Brazil, 19th – 21st October 2005

[5] Rubini, J.J.; Passaro A.; Abe, N. M., & Santos J.C., 2004. Analysis of the electric field distribution in an electrooptic sensor for Pulsed High-Voltage measurements. In: *Fifth IEE International Conference on Computation in Electromagnetics* (*CEM 2004)*, pp. 71-72.

[6] Franco, M.A.R.; Passaro, A.; Sircilli, F., & Cardoso, J.R., 1999. Finite element analysis of anisotropic optical waveguide with arbitrary index profile. *IEEE Transactions on Magnetics*, vol.35, No. 3, pp. 1546-1549.

[7] Abe, N.M.; Franco, M.A.R., & Passaro. A., 1999. *Analysis of a x-cut Ti:LiNbO3 electrooptic modulator with a ridge structure.* In 1999 SBMO/IEEE MTT-S, AP-S and LEOS International Microwave and Optoelectronics Conference (IMOC'99), pp.126-130.

[8] Santos, J.C.; Hidaka, K.; Cortes, A.L.; da Silva, L.P.C., 2003. *Improved optical sensor for high voltage measurement using white light interferometry,* In *2003 SBMO/IEEE MTT-S and LAOS International Microwave and Optoelectronics Conference (IMOC 2003)*, vol.2., pp.615-619.

[9] Santos, J.C. & Hidaka, K.,1997. *Optical high voltage measurement technique using Pockels device*, Japan Journal Appl. Phys., vol. 36, pp. 2394-2398

[10] Santos, J. C. ; Taplamacioglu, M. C. ; Hidaka, K . Pockels High Voltage Measurement System.. In: Eleventh International Symposium on (Conf. Publ. No. 467), 1999. v. 1. p. 53-57.

[11] Pinheiro, L.C.S.; Santos, J.C.; Côrtes A. L., & Hidaka, K., 2002. *Optical high voltage measurement transformer using white light interferometry.* In *25th Brazilian Meeting for Condensed Matter Physic*. pp 204-207

[12] Passaro A.; Rubini, J.J.; Abe, N. M.; Sasaki, M.; SANTOS, J.C. *Finite-Element and Genetic Algorithm Design of Multi-segmented Electro-optic Sensor for Pulsed High-Voltage Measurement*. In: WCSMO6 - 6TH World Congresses of Structural and Multidiscilpinary Optimization, 2005, Rio de Janeiro.

[13] Abe, N.M. et.al., 2002. *Um sistema de software para análise de dispositivos e componentes de óptica integrada, fibras ópticas e microondas.* In V Congresso Brasileiro de Eletromagnetismo (CBMAG 2002*)*, CD-ROM.

[14] Silvester P. P. & Ferrari R. L., 1990. *Finite Elements for Electrical Engineers*, 2th edition, Cambridge University Press.

[15] Almeida, J.C.J.; Santos, J.C.. *Demodulação Coerente do Sinal de Saída de Transformador de Potencial Óptico.* IEEE Latin America Transactions, vol.3, Issue 5, pp. 47-52, December 2005.http://www.ewh.ieee.org/reg/9/etrans/vol3issue5Dec.2005/Vol3issue5Dec.2005TLA.htm .